Available online at www.sciencedirect.com
ScienceDirect
Polymer 49 (2008) 1972–1980
polymer
www.elsevier.com/locate/polymer

Structural and electronic properties of poly(3-thiophen-3-yl-acrylic acid)

Oscar Bertran [a,*], Elaine Armelin [b,*], Juan Torras [a], Francesc Estrany [c], Mireia Codina [c], Carlos Alemán [b,*]

[a] *Departament d'Enginyeria Química, EUETII, Universitat Politècnica de Catalunya, Pça Rei 15, Igualada 08700, Spain*
[b] *Departament d'Enginyeria Química, E.T.S. d'Enginyers Industrials de Barcelona, Universitat Politècnica de Catalunya, Diagonal 647, Barcelona E-08028, Spain*
[c] *Unitat de Química Industrial, EUETIB, Universitat Politècnica de Catalunya, Comte d'Urgell 187, 08036 Barcelona, Spain*

Received 4 January 2008; received in revised form 20 February 2008; accepted 21 February 2008
Available online 4 March 2008

Abstract

This work presents a combined theoretical and experimental study of poly(3-thiophene-3-yl acrylic acid), a new polythiophene derivative soluble in polar solvents. Quantum chemical calculations on small oligomers were performed to propose a structural model for this polymer. Specifically, the minimum energy conformations and the rotational profiles of the different isomeric derivatives constructed for a model system formed by two monomeric units were calculated. The resulting model, which shows head-to-tail polymer linkages and the acrylic acid side group arranged in *trans*-conformation, were used to predict the $\pi-\pi^*$ lowest transition energy of an infinite polymer chain. On the other hand, the polymer was prepared by chemical oxidative coupling using anhydrous ferric chloride and subsequent alkaline hydrolysis. The synthetized material, which is soluble in aqueous base and acetone solutions, was characterized by FTIR, ^{1}H NMR and UV–vis experiments. Both the structural information and electronic properties derived from such experiments are fully consistent with the theoretical model obtained using quantum mechanical calculations.

Keywords: Polythiophene; Transition energy; Computer modeling

1. Introduction

Polythiophene (PTh) is an important class of π-conducting polymers due to their many interesting electronic and optical properties [1,2]. However, unsubstituted PTh is insoluble and infusible due to the rigidity of the backbone and strong intermolecular interactions, *i.e.* recent computer simulation studies proved that the strength of the cohesive forces is remarkably high in PTh [3]. Soluble forms of PTh can be prepared by the introduction of substituents. Specifically, long alkyl side chains increases the solubility in organic solvents [4–6], whereas hydrophilic substituents may produce water-soluble PThs [7–11]. Thus, substituents reduce polymer···polymer intermolecular interactions and increases polymer···solvent interactions. The side chains can also be chosen so that soluble polymers can be rendered insoluble after chemical or photochemical reaction [12]. This transition allows for the spatial disposition of π-conducting polymers in device fabrication.

In a recent study, we modelled the structural and electronic properties of a new PTh derivative with a conjugated substituent, which was produced and characterized in our laboratories [13]. This is poly(3-thiophen-3-yl-acrylic acid methyl ester), abbreviated PT3AME (Scheme 1), in which the electron-withdrawing methylcarboxylate group is separated from the polymer backbone by a double bond. The acrylate substituent was used in the past to promote crosslinking of the polymer chains for controlled hardening of polymers as well as to

* Corresponding authors.
E-mail addresses: oscar@euetii.upc.edu (O. Bertran), elaine.armelin@upc.edu (E. Armelin), carlos.aleman@upc.edu (C. Alemán).

0032-3861/$ - see front matter © 2008 Elsevier Ltd. All rights reserved.
doi:10.1016/j.polymer.2008.02.036

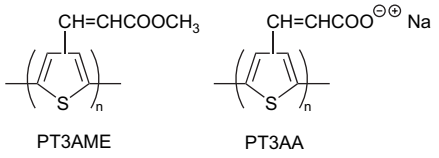

Scheme 1.

functionalize the backbone of the π-conducting polymer with a group amenable of further functionalizations [14–16]. However, in our case we used the acrylate substituent to improve the solubility of PTh as well to enlarge the electronic conjugation from the backbone π-system to the side chain. Interestingly, PT3AME was found to be soluble in a variety of polar organic solvents like acetone and DMSO but it was insoluble in water. Nevertheless, its π–π* lowest transition energy (ε_g), which was determined experimentally (2.54 and 2.48 eV in acetone and DMSO, respectively) and theoretically (2.20 eV), was higher than that obtained for unsubstituted PTh, *i.e.* the ε_g of PTh determined using theoretical [17] and experimental [18,19] methods is 1.82 and ~2.0 eV, respectively.

In this work, we extend our previous study on PT3AME to poly(3-thiophen-3-yl-acrylic acid), hereafter abbreviated PT3AA (Scheme 1). The latter polymer has been prepared from alkaline hydrolysis of the former one, this chemical process transforming the ester groups of PT3AME into ionised carboxylate groups. Furthermore, one of the most relevant characteristics of PT3AA is its solubility in aqueous base solutions, which confers very promising technological properties to this material. Specifically, in this study the molecular structure and conformation of PT3AA have been modelled using quantum mechanical calculations. The resulting model has been used to predict the ε_g value, which has been compared with that determined experimentally using UV–vis spectroscopy. For this purpose, the material was prepared and characterized by FTIR and ^{1}H NMR. Finally, results have been compared with those obtained for PT3AME [13], the influence of the esterification on the structural and electronic properties of this interesting family of PTh derivatives being analyzed.

2. Methods

2.1. Computational methods

In all calculated species, the carboxylate groups were considered in the ionised (deprotonated) state. Full geometry optimizations of oligomers containing *n* monomeric units (*n*-T3AA) with *n* ranging from 2 to 6 were performed using the Unrestricted Hartree–Fock (UHF) method combined with the 6-31+G(d,p) basis set [20], *i.e.* UHF/6-31+G(d,p) level. Previous studies indicated that this basis set is able to provide a very satisfactory description of the molecular geometry and relative energy of negatively charged compounds like those studied in this work [21–23]. On the other hand, UHF calculations describe satisfactorily the molecular geometries of π-conjugated systems, while Density Functional Theory (DFT) calculations tend to overestimate the rotational barriers [24]. Calculations on 2-T3AA were carried out considering three isomeric derivatives that differ in the relative positions of the substituents (Scheme 2). These isomers, which have been denoted as 2-T3AA(4,4′), 2-T3AA(3,3′) and 2-T3AA(3,4′), must be considered as model compounds of the tail-to-tail, head-to-head and head-to-tail polymer linkages, respectively.

The minimum energy conformations of each isomer were determined from full optimizations using a gradient method. For this purpose, all the possible arrangements of the acrylic acid side groups were considered. Furthermore, the internal rotation of the selected arrangements of 2-T3AA(4,4′), 2-T3AA(3,3′) and 2-T3AA(3,4′) isomers was studied by scanning the inter-ring dihedral angle S–C–C–S (θ) in steps of 15° between $\theta = 0°$ (*syn* conformation) and $\theta = 180°$ (*anti* conformation). A flexible rotor approximation was used, each point of the path being obtained from a geometry optimization of the molecule at the UHF/6-31+G(d,p) level considering a fixed value of θ.

The Koopmans' theorem [25] was used to estimate the ionization potentials (IPs). Accordingly, IPs were taken as the negative of the highest occupied molecular orbital (HOMO) energy, *i.e.* $IP = -\varepsilon_{HOMO}$. The IP indicates that a given acceptor (p-type dopant) is capable of ionizing, at least partially, the molecules of the compound. The ε_g was approximated as the difference between the HOMO and lowest unoccupied molecular orbital (LUMO) energies, *i.e.* $\varepsilon_g = \varepsilon_{LUMO} - \varepsilon_{HOMO}$. Although UHF calculations provide a satisfactory qualitative description of the electronic properties of polyheterocyclic molecules, we are aware that this method tends to overestimate the values of IP and ε_g [26,27]. Accordingly, the electronic properties presented in this work have been estimated performing single point DFT calculations with the UB3PW91 [28,29] method combined with the 6-31+G(d,p) basis set [20], *i.e.* UB3PW91/6-31+G(d,p), on the molecular geometries optimised at the UHF/6-31+G(d,p) level. Electronic properties predicted by this methodological combination and experimental values are expected to be quantitatively comparable. Previous studies on π-polyconjugated systems indicated that UB3PW91 is able to reproduce very satisfactorily a wide number of electronic

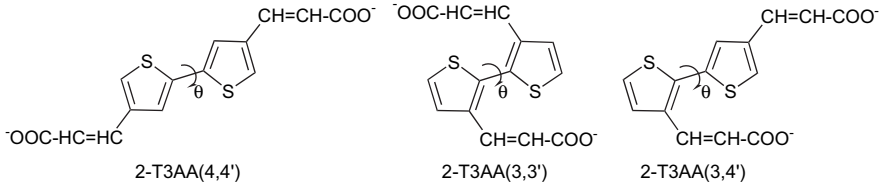

Scheme 2.

properties [13,17,30,31]. It is worth noting that according to the Janak's theorem [32], the approximation mentioned above for the calculation of the IP can be applied to DFT calculations, while Levy and Nagy evidenced that ε_g can be rightly approximated as the difference between ε_{LUMO} and ε_{HOMO} in DFT calculations [33].

All the quantum mechanical calculations presented in this work were performed using the Gaussian 03 computer program [34].

2.2. Experimental methods

3-Thiophen-3-yl-acrylic acid (T3AA) and anhydrous ferric chloride were purchased from Sigma–Aldrich Química S.A. and were employed without further purification. All solvents were purchased from Panreac Química S.A. with ACS grade.

FTIR spectra were recorded on a 4100 Jasco spectrophotometer equipped with an ATR MKII Golden Gate Heated Single Reflection Diamond Specac model. The UV–vis optical spectrum of the polymer was obtained from its 1 mg/mL solution in aqueous base using a Shimadzu UV-240 Graphtcord UV–vis recording spectrophotometer. Proton NMR spectra of the monomer and polymer were recorded on a Varian Inova 300 spectrometer operating at 300.1 MHz. For this purpose, they were dissolved in deuterated chloroform ($CDCl_3$) and the chemical shifts were calibrated using tetramethylsilane as internal standard.

3. Results and discussion

3.1. Modeling the dimeric units: minimum energy conformations and rotational profiles of 2-T3AA

It should be noted that the acrylic acid group attached to the thiophene rings of 2-T3AA(4,4′), 2-T3AA(3,3′) and 2-T3AA(3,4′) can adopt different arrangements, which are expected to affect the conformational preferences of this compound. These arrangements are consequence of both the orientation of the whole side group and the *trans* ↔ *cis* isomerism of the acrylic acid double bond.

The nomenclature used to define all the possible arrangements of the side chains is defined in Scheme 3: *t* and *c* refer to the *trans* and *cis* arrangements of the double bond, respectively, while *n* and *r* denote the orientation of the first hydrogen atom of the acrylic acid side group. Thus, *n* indicates that such hydrogen is oriented towards the sulphur atom of the neighbouring thiophene ring, while *r* refers to the opposite orientation. Accordingly, four different possibilities can be defined for each substituent: *tr*, *tn*, *cr* and *cn* (see Scheme 3).

Table 1
Minimum energy conformations considering different arrangements of the side groups calculated for the 2-T3AA(4,4′) isomer at the UHF/6-31+G(d,p) level

2-T3AA(4,4′)[a]	*anti–gauche*	*syn–gauche*
tr–tr	0.0 ($\theta = 152.0°$)	2.6 ($\theta = 58.5°$)
tr–tn	0.7 ($\theta = 150.3°$)	2.5 ($\theta = 51.2°$)
tr–cr	7.6 ($\theta = 156.7°$)	–
tr–cn	4.3 ($\theta = 147.6°$)	4.6 ($\theta = 44.7°$)
tn–tn	1.3 ($\theta = 149.4°$)	2.7 ($\theta = 48.4°$)
tn–cr	8.5 ($\theta = 153.6°$)	10.9 ($\theta = 55.7°$)
tn–cn	4.6 ($\theta = 148.5°$)	5.1 ($\theta = 45.1°$)
cr–cr	16.0 ($\theta = 162.8°$)	–
cr–cn	13.5 ($\theta = 145.6°$)	13.2 ($\theta = 39.1°$)
cn–cn	7.7 ($\theta = 149.4°$)	8.3 ($\theta = 47.3°$)

Relative energies are in kcal/mol.
[a] See Scheme 3.

Table 1 lists the minimum energy conformations found for 2-T3AA(4,4′) considering all the possible arrangements of the side chain. It is worth noting that due to the chemical and molecular symmetry of this compound, *i.e.* substitutions at C4 and C4′, only 10 of the 16 expected arrangements are actually different, *e.g.* the arrangement with the side groups in *tr* and *tn* (*tr–tn*) is equivalent to that with the side groups in *tn* and *tr* (*tn–tr*). All the arrangements show an *anti–gauche* minimum with θ ranging from 146° to 163°, even though the relative energy of three of them only was lower than 1.5 kcal/mol. These correspond to *tr–tr*, *tr–tn* and *tn–tn*, the former being the global minimum and the latter two being unfavored by 0.7 and 1.3 kcal/mol, respectively. On the other hand, all the arrangements with exception of *tr–cr* and *cr–cr* show a *syn–gauche* local minimum, whose relative energy ranges from 2.5 to 10.9 kcal/mol.

In order to get a deeper insight into the conformational properties of 2-T3AA(4,4′), we examined the internal rotation of this isomer considering three different arrangements for the acrylic acid side groups (Scheme 4): (i) the *tr–tr*, which corresponds to the global minimum; (ii) the *tr–cn*, which is the lowest energy arrangement with one side group in *trans* and the other in *cis* (Table 1); and (iii) the *cn–cn*, which is the lowest energy arrangement with the two side groups in *cis* (Table 1).

Fig. 1 shows the UHF/6-31+G(d,p) energy profiles of 2-T3AA(4,4′)/*tr–tr*, 2-T3AA(4,4′)/*tr–cn* and 2-T3AA(4,4′)/*cn–cn* relative to the most stable conformation. Furthermore, the position and energy of both the minimum energy conformations and the barriers are summarized in Table 2. As can be seen, 2-T3AA(4,4′)/*tr–cn* and 2-T3AA(4,4′)/*cn–cn* have the less favored profiles due to the unfavourable steric interactions between the acrylic acid side groups arranged in *cis* and the hydrogen atoms attached to the C5 atom of the thiophene

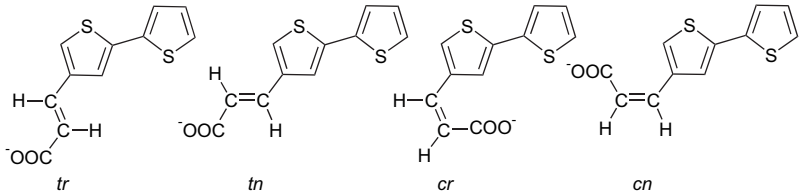

Scheme 3.

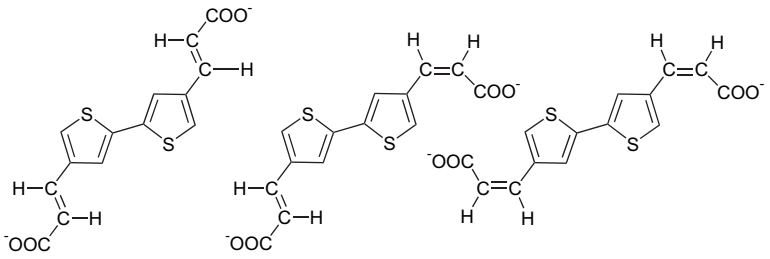

Scheme 4.

rings. As a consequence, these arrangements are about 4–6 kcal/mol and 7.5–10 kcal/mol, respectively, less favored than the 2-T3AA(4,4′)/*tr*–*tr* one. On the other hand, it is worth noting that, in spite of the ionised nature of the substituents, the three profiles displayed in Fig. 1 for 2-T3AA(4,4′) are similar to those typically found for unsubstituted 2,2′-bithiophene as well as its derivatives bearing neutral substituents in positions 4 and 4′ [17,24,35,36]. Thus, in all the cases the minima are located at the *anti*–*gauche* ($\theta \approx 150°$) and *syn*–*gauche* ($\theta \approx 50°$) conformations, while the *syn* ($\theta = 0°$), *gauche*–*gauche* ($\theta \approx 90°$) and *anti* ($\theta = 180°$) rotamers are energy barriers.

Table 3 lists the energies, which are relative to the global minimum of 2-T3AA(4,4′) of the *anti*–*gauche* minima found for the 2-T3AA(3,3′) isomer. As can be seen, the arrangements with at least one side group oriented in *cr* (see Scheme 3) were not stable due to repulsive steric interactions. Interestingly, substitutions at C3 and C3′ produced not only a significant reduction in the value of θ, which ranged from 101° to 121°, but also a significant destabilization of the minimum energy conformations. Thus, the energies of the *anti*–*gauche* minima found for 2-T3AA(3,3′) varied from 14 to 23 kcal/mol. On the other hand, no *syn*–*gauche* minimum was identified for the arrangements investigated.

Fig. 2 displays the rotational profiles calculated for the *tn*–*tn* and *tn*–*cn* arrangements of the 2-T3AA(3,3′) isomer (Scheme 5), which show the *anti*–*gauche* minima of lower energy (Table 3). The relative energies of the profile are calculated with respect to the lowest energy minimum of the 2-T3AA(4,4′)/*tr*–*tr*, which corresponds to the global minimum. It is worth noting that the relative energies provided by the arrangements with the two side groups arranged in *cis* were so high that the calculation of their rotational profiles was not considered necessary. On the other hand, the relative energies predicted for the minimum energy conformations and the energy barriers are included in Table 2.

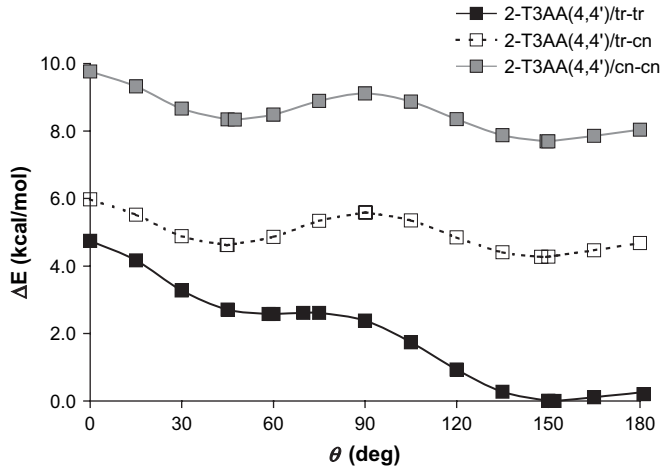

Fig. 1. Potential energy curves for the internal rotation of 2-T3AA(4,4′)/*tr*–*tr*, 2-T3AA(4,4′)/*tr*–*cn* and 2-T3AA(4,4′)/*cn*–*cn* as a function of the inter-ring dihedral angle (θ) using UHF/6-31+G(d,p) geometry optimizations. Energies are relative to the global minimum.

Table 2
Relative energies[a] (kcal/mol) and inter-ring dihedral angles (θ) of the minimum energy conformations and barriers calculated for selected arrangements of the 2-T3AA(4,4′), 2-T3AA(3,3′) and 2-T3AA(4,4′) isomers at the UHF/6-31+G(d,p) level

#	*syn*[b]	*syn*–*gauche*	*gauche*–*gauche*[c]	*anti*–*gauche*	*anti*[d]
2-T3AA(4,4′)/*tr*–*tr*	4.7	2.6 ($\theta = 58.5°$)	2.4	0.0[e] ($\theta = 152.0°$)	0.2
2-T3AA(4,4′)/*tr*–*cn*	6.0	4.6 ($\theta = 44.7°$)	5.6	4.3 ($\theta = 147.6°$)	4.7
2-T3AA(4,4′)/*cn*–*cn*	9.8	8.3 ($\theta = 47.3°$)	9.1	7.7 ($\theta = 149.4°$)	8.0
2-T3AA(3,3′)/*tn*–*tn*	43.3	–	–	13.9 ($\theta = 120.8°$)	18.9
2-T3AA(3,3′)/*tn*–*cn*	37.7	–	–	16.4 ($\theta = 112.1°$)	24.5
2-T3AA(3,4′)/*tn*–*tr*	18.3	–	–	7.7 ($\theta = 136.3°$)	9.2

[a] Energies are relative to the global minimum of 2-T3AA(4,4′).
[b] $\theta = 0.0°$.
[c] $\theta = 90.0°$.
[d] $\theta = 180.0°$.
[e] $E = -1629.328770$ a.u.

Table 3
Minimum energy conformations considering the different arrangements of the side groups calculated for the 2-T3AA(3,3′) isomer at the UHF/6-31+G(d,p) level

2-T3AA(3,3′)[a]	*anti*–*gauche*
tr–*tr*	23.1 ($\theta = 116.9°$)
tr–*tn*	18.4 ($\theta = 119.6°$)
tr–*cn*	21.5 ($\theta = 111.4°$)
tn–*tn*	13.8 ($\theta = 120.8°$)
tn–*cn*	16.6 ($\theta = 110.6°$)
cn–*cn*	17.8 ($\theta = 101.4°$)

Relative energies are in kcal/mol.
[a] See Scheme 3.

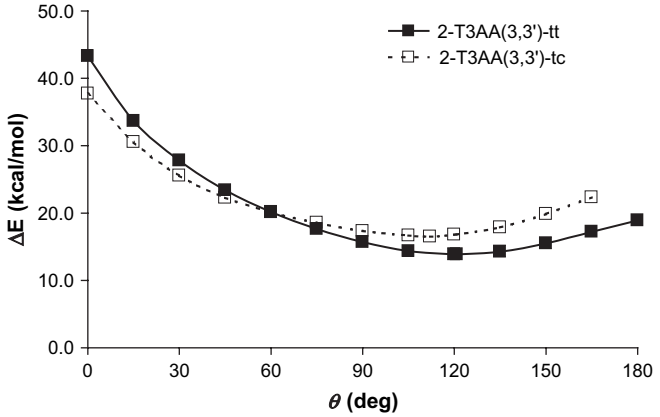

Fig. 2. Potential energy curves for the internal rotation of 2-T3AA(3,3′)/*tn*−*tn* and 2-T3AA(3,3′)/*tn*−*cn* as a function of the inter-ring dihedral angle (θ) using UHF/6-31+G(d,p) geometry optimizations. Energies are relative to the global minimum of the 2-T3AA(4,4′) isomer.

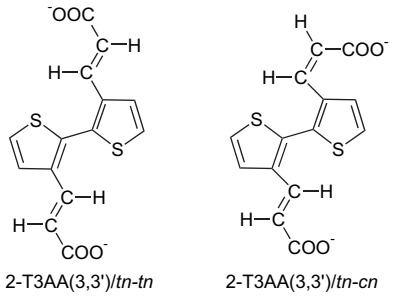

Scheme 5.

The shape of the rotational profiles calculated for 2-T3AA(3,3′)/*tn*−*tn* and 2-T3AA(3,3′)/*tn*−*cn* is completely different from that obtained for the three arrangements of the 2-T3AA(4,4′) isomer (Fig. 1). This is because the repulsive interactions produced by substitution at the C3-position are strong enough to induce drastic changes in the conformational preferences. Thus, the energies listed in Table 2, which are relative to the global minimum of the most stable arrangement of 2-T3AA(4,4′), indicate that the latter isomer is around 14–16 kcal/mol more stable than 2-T3AA(3,3′). The main conformational features observed for the 2-T3AA(3,3′) isomer can be summarized as follows: (i) a single minimum appears at $\theta \approx 112-120^\circ$ and no local minimum being detected in the *syn*−*gauche* region; (ii) the *syn* and *anti* barriers are destabilized by about 21–29 kcal/mol and 5–8 kcal/mol, respectively, while the *gauche*−*gauche* is not an energy barrier. Furthermore, it is worth noting that the potential energy surface $E = E(\theta)$ is very flat in the range from $\theta \approx 75^\circ$ to 150°, where the repulsive interactions generated by the side groups attached to C3 are minimized. In contrast, such unfavourable interactions become maxima when the molecule adopts a planar *syn* conformation.

Table 4 displays the minimum energy conformations found for the different arrangements of 2-T3AA(3,4′). It is worth noting that 16 arrangements were considered in this case due to the lack of molecular symmetry in this isomer. Interestingly, no arrangement was stable when the substituent attached to C3 adopts a *cr* orientation, this feature being fully consistent with the results

Table 4
Minimum energy conformations considering the different arrangements of the side groups calculated for the 2-T3AA(3,4′) isomer at the UHF/6-31+G(d,p) level

2-T3AA(4,4′)[a]	*anti*−*gauche*	*syn*−*gauche*
tr−*tr*	12.5 ($\theta = 137.2^\circ$)	–
tr−*tn*	13.4 ($\theta = 131.7^\circ$)	–
tr−*cr*	20.1 ($\theta = 140.6^\circ$)	–
tr−*cn*	18.4 ($\theta = 114.6^\circ$)	18.2 ($\theta = 48.0^\circ$)
tn−*tr*	7.7 ($\theta = 136.4^\circ$)	–
tn−*tn*	8.6 ($\theta = 132.7^\circ$)	–
tn−*cr*	15.3 ($\theta = 138.0^\circ$)	–
tn−*cn*	13.6 ($\theta = 115.8^\circ$)	12.7 ($\theta = 43.8^\circ$)
cn−*tr*	9.1 ($\theta = 120.6^\circ$)	–
cn−*tn*	9.8 ($\theta = 113.8^\circ$)	–
cn−*cr*	18.0 ($\theta = 120.5^\circ$)	–
cn−*cn*	–	13.41 ($\theta = 56.8^\circ$)

Relative energies are in kcal/mol.
[a] See Scheme 3.

obtained for the 2-T3AA(3,3′) isomer. On the other hand, only three arrangements (*tr*−*cn*, *tn*−*cn* and *cn*−*cn*) show a *syn*−*gauche* minimum, while the *cn*−*cn* one is not able to adopt an *anti*−*gauche* conformation. The relative energies ranging from 7 to 20 kcal/mol indicates that, in general, the stability of this isomer is between those of 2-T3AA(4,4′) and 2-T3AA(3,4′).

The only rotational profile calculated for the 2-T3AA(3,4′) isomer corresponds to the *tn*−*tr* orientation of the acrylic acid substituents (Scheme 6) since its *anti*−*gauche* minimum (Table 4) is significantly more stable than that of the other arrangements.

The rotational profile is displayed in Fig. 3, in which energies are relative to that of the lowest energy minimum obtained for 2-T3AA(4,4′)/*tr*−*tr*. On the other hand, information about both the minimum and energy barriers is included in Table 2. As can be seen, the minimum appears at $\theta = 136^\circ$, the *anti* barrier being unfavored by only 1.5 kcal/mol. In contrast, the *syn* barrier shows strong steric contacts that lead to a destabilization of 13.6 kcal/mol. The main differences between the profile obtained for 2-T3AA(3,4′)/*tn*−*tr* and those calculated for the 2-T3AA(4,4′) isomer correspond to the elimination of the *syn*−*gauche* minimum and the *gauche*−*gauche* barrier.

3.2. Modeling the polymer: prediction of the electronic properties of PT3AA

The lowest energy minimum of 2-T3AA was obtained for the isomer with acrylic acid side group attached to C4 and

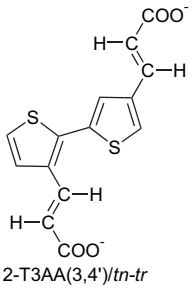

Scheme 6.

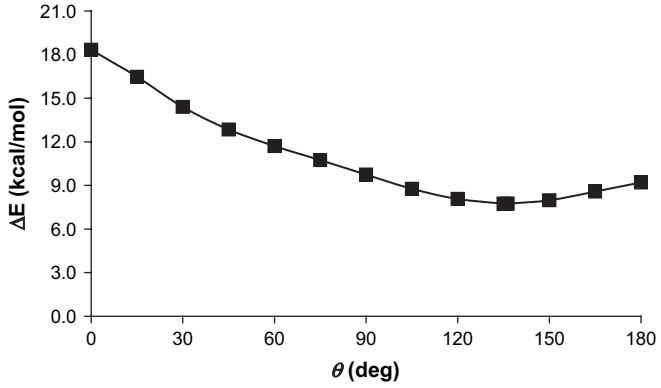

Fig. 3. Potential energy curves for the internal rotation of 2-T3AA(3,4′)/*tn*−*tr* as a function of the inter-ring dihedral angle (θ) using UHF/6-31+G(d,p) geometry optimizations. Energies are relative to the global minimum of the 2-T3AA(4,4′) isomer.

C4′. However, it should be noted that the construction of a model by polymerizing the 2-T3AA(4,4′) isomer gives place to an alternated sequence of tail-to-tail and head-to-head linkages (Scheme 7). In the previous section, we found that the latter type of linkage, which was represented by the 2-T3AA(3,3′) isomer, produces very unstable structures. Therefore, the construction of a model for PT3AA based on alternated head-to-head and tail-to-tail linkages was discarded because the stability of the 2-T3AA(4,4′) isomer is largely surpassed by the high unstability of the 2-T3AA(3,3′) isomer.

On the other hand, calculations on 2-T3AA(3,4′) indicated that a minimum energy conformation with a relatively low energy is obtained when the side groups adopt a *tn*−*tr* arrangement (Table 2). Accordingly, we used the 2-T3AA(3,4′)/*tn*−*tr* structure to construct a model in which head-to-tail polymer linkages are repeated along the chain (Scheme 8). This situation is significantly more stable than that formed by alternating tail-to-tail and head-to-head polymer linkages. This head-to-tail model was used to build oligomers containing n monomeric units with $n = 2$, 3, 4 and 5, which were optimised at the UHF/6-31+G(d,p) level fixing the inter-ring dihedral angles θ at 180°. Previous studies indicated that, in order to extrapolate the electronic properties calculated for oligomers to infinite chain polymers, conformational effects should be omitted by imposing an all-*anti* conformation [27,37].

Fig. 4 shows the C−C bond-length alternation patterns along the π-system of the backbone for the oligomer with $n = 5$. As can be seen, the geometric structure of this oligomer shows a clear benzenoid character. In order to evaluate the ε_g and IP, single point calculations at the UB3PW91/6-31+G(d,p) level were

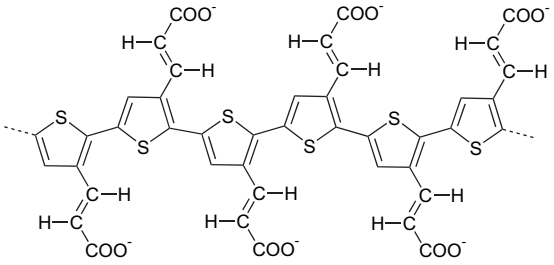

Scheme 8.

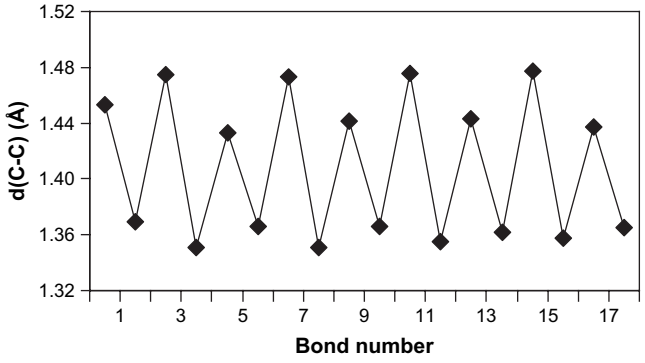

Fig. 4. C−C bond distances along the conjugated π-system of the oligomer with $n = 5$.

performed on the optimised geometries of oligomers containing head-to-tail linkages. Fig. 5 shows the linear behaviors (correlation coefficient $r > 0.98$) for the variation of the calculated ε_g and IP with the inverse chain length ($1/n$). Linear regression analyses, which are also displayed in Fig. 5, allowed to extrapolate ε_g and IP values of 2.12 and 5.66 eV, respectively, for an infinite chain of PT3AA. It is worth noting that the ε_g of PT3AME (2.20 eV) was predicted to be 0.08 eV larger than that calculated for PT3AA [13]. Indeed, the ε_g obtained in this work for the latter polymer is 0.30 eV larger than that previously computed for PTh (1.82 eV) using the same DFT method [17]. On the other hand, the IP predicted for PT3AA is 0.55 eV larger than that obtained for PT3AME (5.11 eV) [13] indicating that esterification of the carboxylate groups facilitates significantly the p-doping process.

3.3. Comparison with experimental data: synthesis and characterization of PT3AA

3.3.1. Synthesis

T3AA (3 g) was refluxed in dry methanol (15 mL) with one drop of concentrated sulfuric acid for 24 h to provide

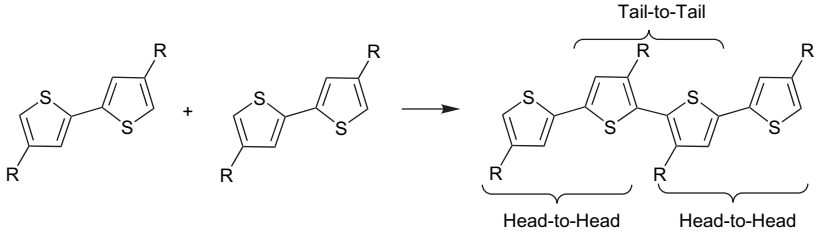

Scheme 7.

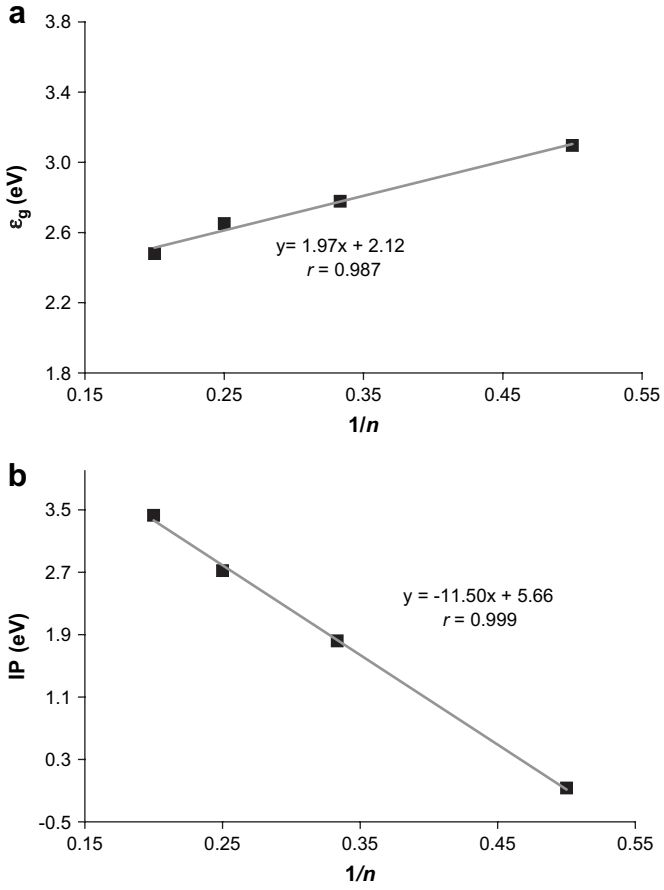

Fig. 5. Variation of (a) ε_g (in eV) and (b) IP (in eV) against $1/n$, where n is the number of monomeric units, for PT3AA. The gray lines correspond to the linear regressions used to obtain the ε_g for infinite chain systems.

3-thiophen-3-yl-acrylic acid methyl ester (T3AME). The purification and extraction of this monomer, which was obtained with 99.9% of yield, were carried out by using the procedure described in our previous work [13]. Polymerization of T3AME to produce PT3AME was performed by chemical oxidative coupling in dry methanol using anhydrous ferric chloride. A detailed description of this process as well as of the purification of the resulting material is provided in Ref. [13]. The transformation of PT3AME into PT3AA was performed by alkaline hydrolysis. Thus, the former polymer (~1 g) was stirred in 100 mL of 2 M NaOH solution for 24 h at 100 °C. The resulting mixture was filtered to remove the insoluble part and was poured into 1 M HCl aqueous solution to precipitate the PT3AA. This material was repeatedly washed with deionized water and dried under vacuum for three days (yield: 81–87%).

3.3.2. Characterization

Fig. 6 compares the FTIR spectrum of PT3AA with that of the monomer T3AA. A detailed analysis of the absorption bands allows us to confirm that the polymer was successfully obtained by chemical oxidative reaction with $FeCl_3$ and subsequent alkaline hydrolysis. The bands higher than 3000 cm^{-1} typically detect unsaturated compounds if the stronger main bands associated to hydrogen bonds formed by acid or alcohol

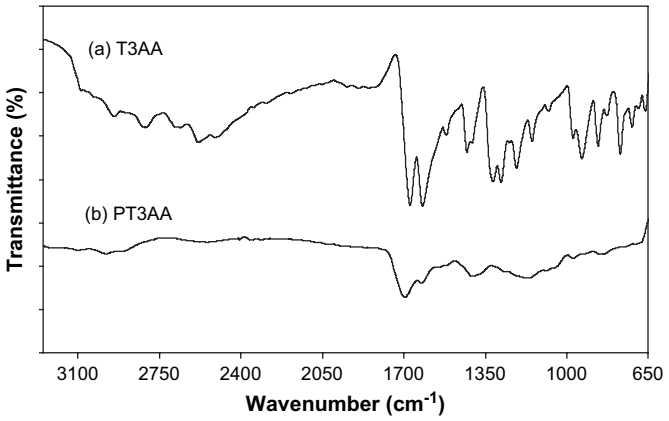

Fig. 6. FTIR spectrum of (a) 3-thiophen-3-yl-acrylic acid (T3AA) and (b) poly(thiophen-3-yl-acrylic acid) (PT3AA).

groups do not hide them. According to Ruiz et al. [38], the absorbance due to the aromatic C–H stretch at ~3070 cm^{-1} can be attributed to the β-hydrogen whereas the band at ~3090 cm^{-1} is related to the α-hydrogen position in the thiophene rings. These absorbances could not be identified in Fig. 6 because of the broad band from OH group detected between 3300 and 2500 cm^{-1}. On the other hand, the β C–H out-of-plane deformation was observed as a medium peak at 866 cm^{-1} while the α C–H out-of-plane deformation appears as a very sharp band at 771 cm^{-1}. As we can be seen in the FTIR spectrum of PT3AA, the strong peak at about 771 cm^{-1} related to the α C–H out-of-plane deformation disappears indicating that the α positions (2,5 positions, alternatively) of thiophene ring have been successfully attached.

The most characteristic feature in the PT3AA spectrum is the broad absorption occurring in the region from 1500 to 1650 cm^{-1} that corresponds to the conjugated C=C stretching absorbance, being also a proof of polymerization. Moreover, the conjugated double bond associated to the acrylic acid side group is found in the ~1630 cm^{-1} region, and the mode of substitution is identified by the C–H out-of-plane bending bands at 976 and 848 cm^{-1}. In our previous work [13] we proved that the *trans*-conformation of the acrylic acid conjugated double bond is maintained in the esterification process and polymerization step. This is in good agreement with the theoretical predictions presented in the previous section.

Although PT3AA is completely insoluble in the common organic solvents and neutral water, it dissolves completely in aqueous base solutions, *i.e.* pH 10–12, and acetone. Fig. 7 shows the UV spectra recorded for PT3AA in aqueous base solution and acetone. The first absorption band on the low energy side of the spectra arises from the π–π* transition in the delocalized electron system along the chain. Thus the energy of the band gap of the conduction can be estimated from the intersection of a tangent placed over the inflection point of this curve and the wavelength axes. The broad absorption band displayed in the spectra is the result of a serial of different higher energy intra- and inter-chain electron transitions in the polymer matrix. The ε_g values estimated from the UV–vis spectra in aqueous base and acetone solutions are 2.34 and 2.45 eV, respectively, indicating that the energy

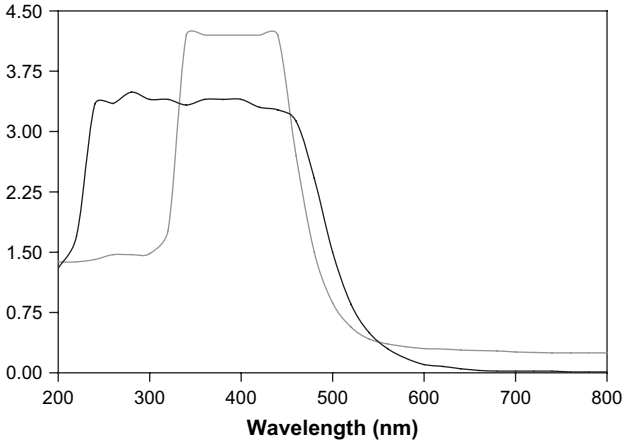

Fig. 7. UV–vis spectra of poly(3-thiophen-3-yl-acrylic acid) (PT3AA) in aqueous base solution (black line) and acetone (gray line).

required by the π–π* transition decreases with the polarity of the environment. These gaps are only 0.22 and 0.33 eV larger than that predicted by theoretical calculations. A similar underestimation of the ε_g by DFT calculations was found for PTh (experimental and theoretical values of ε_g are ~2.0 and 1.82 eV, respectively [18,19]) and PT3AME (experimental and theoretical values of ε_g are ~2.5 and 2.20 eV, respectively [13]). The overall of these results indicate that DFT calculations provide very reliable estimations of the gap, the small underestimation being attributed to the omission of the environmental effects and structural defects in the theoretical model. On the other hand, comparison between the ε_g values determined for PT3AA and PT3AME [13] from the UV–vis spectra recorded in acetone solution (2.45 and 2.54 eV, respectively) reveals that alkaline hydrolysis of the ester groups produces a small reduction of the gap.

Finally, the molecular structures of monomers and polymers studied in this work were determined by ^{1}H NMR spectroscopy (data not shown), results being in agreement with the modelled chemical structures. Thus, the coupling constant of the −CH=CH− protons in the acrylic acid group of T3AA monomer was calculated to be $J = 15.9$ Hz corroborating the results obtained by IR spectroscopy, *i.e.* the *trans* geometry of the conjugated double bond is maintained after the esterification reaction. Furthermore, the esterification and hydrolysis steps were confirmed by the corresponding appearance and disappearance of $-COOCH_3$ and −OH signals.

On the other hand, the splitting of the $-COOCH_3$ signal in PT3AME can be used to obtain information about the ratio of head-to-tail and head-to-head diads arising from polymerization [2]. For poly(3-dodecylthiophene) the resonance for a head–head coupling is observed at $\delta = 2.56$ ppm while that of a head-to-tail coupling appears at $\delta = 2.79$ ppm (protons on the α-carbon of the 3-position) [2]. It should be noted that in our previous work we reported an accurate analysis of the proton peak areas in the 3.7–3.0 ppm region for PT3AME. Results showed that ~80% of the diads are head-to-tail [13]. This predominance is in excellent agreement with the model proposed in the previous section for PT3AA.

4. Conclusions

Quantum mechanical calculations have been used to examine both the minimum energy conformations and the rotational profiles of the three isomers of 2-T3AA in the unionised state. Results indicate that the rotational profiles of 2-T3AA(4,4′) are similar to those obtained for unsubstituted 2,2′-bithiophene, while 2-T3AA(3,3′) and 2-T3AA(3,4′) deviate significantly from such behavior. The lowest energy conformation of 2-T3AA was obtained for the isomer with the two acrylic acid substituents arranged in *tr–tr* and attached to the C4 and C4′ positions. In contrast, the stability of the 2-T3AA(3,3′) isomer was very low, a few minima with very high relative energies being obtained in this case. The model developed for the PT3AA was based on the lowest energy arrangement of the 2-T3AA(3,4′) isomer. This model is based on head-to-tail polymer linkages and *tn* and *tr* arrangements for the acrylic acid substituent disposed alternatively. The π–π* lowest transition energy predicted using this model is 2.12 eV, which is higher than that previously computed for PTh (1.82 eV) but slightly lower than that calculated for PT3AME (2.20 eV).

On the other hand, PT3AA has been synthetized using the same synthetic route previously used to prepare PT3AME [13], the latter being transformed into the former by alkaline hydrolysis. The π–π* lowest transition of this polymer, which is soluble in aqueous base and acetone solutions, was determined from the recorded UV–vis spectra. The ε_g values are 2.34 and 2.45 eV in aqueous base and acetone solutions, respectively. As can be seen, there is an excellent agreement between theoretical and experimental values, *i.e.* ε_g values calculated using DFT methods are typically underestimated by 0.2–0.3 eV with respect to the measured ones. Similarly, the structural information obtained using both FTIR and ^{1}H NMR is fully consistent with that provided by quantum mechanical calculations.

Acknowledgements

This work has been supported by MCYT and FEDER with Grant MAT2006-04029. Authors are indebted to the Centre de Supercomputació de Catalunya (CESCA) for computational facilities.

References

[1] Roncali J. Chem Rev 1997;97:173.
[2] Skotheim TA, Reynolds JR. Handbook of conducting polymers. 3rd ed. Boca Raton: CRC Press; 1998.
[3] Curcó D, Alemán C. J Comput Chem 2007;28:1743.
[4] Chen TA, Wu X, Rieke RD. J Am Chem Soc 1995;117:233.
[5] Souto Maior RM, Hinkelman K, Eckert H, Wudl F. Macromolecules 1990;23:1268.
[6] Demanze F, Yassar A, Garnier F. Adv Mater 1995;7:907.
[7] Kim B, Chen L, Gong J, Osada Y. Macromolecules 1999;32:3964.
[8] Rasmussen SC, Pickens JC, Hutchison JE. Macromolecules 1998;31:933.
[9] Rasmussen SC, Pickens JC, Hutchison JE. Chem Mater 1998;10:1990.
[10] McCullough RD, Ewbank PC, Loewe RS. J Am Chem Soc 1997;119:633.

[11] Ewbank PC, Loewe RS, Zhai L, Reddinger J, Sauve G, McCullough R. Tetrahedron 2004;60:11269.
[12] Lowe J, Holdcroft S. Macromolecules 1995;28:4608.
[13] Betran O, Pfeiffer P, Torras J, Armelin E, Estrany F, Alemán C. Polymer 2007;48:6955.
[14] Zotti G, Berlin A. Synth Met 1999;105:135.
[15] Lankinen E, Sundholm P, Talonen H, Grano F, Sundholm J. Electroanal Chem 1999;460:176.
[16] Dock TJJM, de Ruiter B. Synth Met 1996;79:215.
[17] Casanovas J, Zanuy D, Alemán C. Polymer 2005;46:9452.
[18] Kobayashi M, Chem J, Chung T-C, Moraes F, Heeger AJ, Wudl F. Synth Met 1984;9:77.
[19] Chung T-C, Kaufman JH, Heeger AJ, Wudl F. Phys Rev B 1984;30:702.
[20] McLean AD, Chandler GS. J Chem Phys 1980;72:5639.
[21] Alemán C. J Phys Chem A 2000;104:7612.
[22] Alemán C, Zanuy D. Chem Phys Lett 2000;319:318.
[23] Alemán C, Zanuy D. Chem Phys Lett 2001;343:390.
[24] Alemán C, Domingo VM, Fajarí L, Juliá L, Karpfen A. J Org Chem 1998;63:1041.
[25] Koopmans T. Physica 1934;1:104.
[26] Gatti C, Frigerio G, Benincori T, Brenna E, Sannicolò F, Zotti G, et al. Chem Mater 2000;12:1490.
[27] Alemán C, Armelin E, Iribarren JI, Liesa F, Laso M, Casanovas J. Synth Met 2005;149:151.
[28] Becke AD. J Chem Phys 1993;98:1372.
[29] Perdew JP, Wang Y. Phys Rev B 1992;45:13244.
[30] Casanovas J, Alemán C. J Phys Chem C 2007;111:4823.
[31] Alemán C, Casanovas J. J Phys Chem A 2004;108:1440.
[32] Janak JF. Phys Rev B 1978;18:7165.
[33] Levy M, Nagy A. Phys Rev A 1999;59:1687.
[34] Frisch MJ, Trucks GW, Schlegel HB, Scuseria GE, Robb MA, Cheeseman JR, et al. Gaussian 03, Revision B.02. Pittsburgh, PA: Gaussian, Inc.; 2003.
[35] Alemán C, Juliá L. J Phys Chem 1996;100:1524.
[36] Ocampo C, Alemán C, Curcó D, Casanovas J. Synth Met 2006;156:602.
[37] Ocampo C, Casanovas J, Liesa F, Alemán C. Polymer 2006;47:3257.
[38] Ruiz JP, Kayak K, Marynick DS, Reynolds JR. Macromolecules 1989;22:1231.